A High-Q Millimeter-Wave Dielectric-Resonator Bandpass Filter Using Whispering-Gallery Modes

Y. Ji,[1] X. S. Yao,[1] and L. Maleki[1]

A low-cost millimeter-wave dielectric-resonator filter using a high-order whispering-gallery mode with the coupling of curved microstrip transmission line has been successfully developed for the mode selection in a millimeter-wave optoelectronic oscillator. The achieved 3-dB bandwidth of this filter is 10.5 MHz (loaded quality factor, Q, is about 3,000) or 0.03 percent at 31.5 GHz with a 3-dB insertion loss and more than a 25-dB band-stop attenuation.

I. Introduction

An optoelectronic oscillator (OEO) recently developed at JPL has the capability to provide an extremely low phase-noise microwave signal by using fiber delay [1]. However, because the OEO is essentially a multimode device and its mode spacing is inversely proportional to the length of the fiber, further reduction of phase noise requires a high quality factor, Q, filter with narrow enough bandwidth to select a mode for operation at a single frequency.

The cavity filter and waveguide filter are designed for high frequency bands and have relatively high Q. Their 3-dB passband widths can be as narrow as 0.1 percent, but generally these filters are bulky and have bad temperature stability for operation modes due to the thermal expansion of metal cavity.

The first challenge of using a dielectric resonator as a filter was given by S. Cohn [2] in 1968. Cohn indicated that dielectric-resonator loaded high-Q narrowband filters can be designed to occupy a total volume of only about 5 percent of that of a waveguide filter with an equivalent performance. J. Arnaud initiated the study of whispering-galley (WG) modes of a dielectric resonator in 1981 [3]. His work shows that WG modes enable designers to use larger-sized dielectric resonators (DRs) at higher frequencies with a possible higher Q. The group led by P. Guillion applied the WG modes to the design of a millimeter-wave band-stop filter [4] and a 12- to 18-GHz (Ku-band) bandpass filter [5] for the first time. However, the achieved loaded Q was only a few hundreds.

---

[1] Tracking Systems and Applications Section.

The research described in this publication was carried out by the Jet Propulsion Laboratory, California Institute of Technology, under a contract with the National Aeronautics and Space Administration.

In this article, we present a new configuration of a millimeter-wave dielectric-resonator filter by using a high-order whispering-gallery mode with a coupling of curved microstrip transmission line. The energy of the high-order whispering-gallery-mode resonator is confined in a very small region close to the boundary surface, and this type of WG mode provides a better opportunity of coupling to planar transmission lines. The achieved 3-dB bandwidth of this filter is 10.5 MHz (loaded Q is about 3,000) or 0.03 percent at 31.5 GHz with a 3-dB insertion loss and more than a 25-dB band-stop attenuation.

II. Whispering-Gallery (WG) Modes of Dielectric Resonators

At frequencies below 20 GHz, low-order modes such as $TE_{01\delta}$ and $TM_{01\delta}$ have found their applications as oscillators, filters, and power combiners [6,7]. These modes can be relatively easily coupled by cut-off waveguides, magnetic loops, and microstrip lines. For a relatively large-sized cylindrical resonator at higher frequencies, say above 30 GHz, whispering-gallery modes, which are believed to have a higher Q but to be more difficult to couple simply with microstrip lines, can be observed. WG modes are classified as transverse electric modes $TE_{n,m,l}$ or $WGE_{n,m,l}$ and transverse magnetic $TM_{n,m,l}$ or $WGM_{n,m,l}$, where "n," "m," and "l" denote the azimuthal, ϕ; radial, r; and axial, z, mode numbers, respectively.

One three-dimensional electromagnetic (EM) field presentation of $TE_{5,1,\delta}$ in the disk plane is shown in Fig. 1, and a ray-tracing model of WG modes is shown in Fig. 2. It is easy to see that most of the EM energy is confined in a small area between the caustic and the cylindrical boundary when the azimuthal mode number, n, is large enough. Using WG modes could help designers easily handle large enough DR disks in the millimeter-wave integrated circuits. In additional, WG modes have higher Q values, which are only limited by the material loss.

Since TE modes have transverse electric fields, or $E_z = 0$, the essential field components are H_z, E_r, and E_ϕ. As shown in the following Maxwell equations, E-field components can be expressed from the H-field:

$$E_r = \frac{1}{j\omega\varepsilon_r r}\frac{\partial H_z}{\partial \phi} \tag{1a}$$

and

$$E_\phi = -\frac{1}{j\omega\varepsilon_r}\frac{\partial H_a}{\partial r} \tag{1b}$$

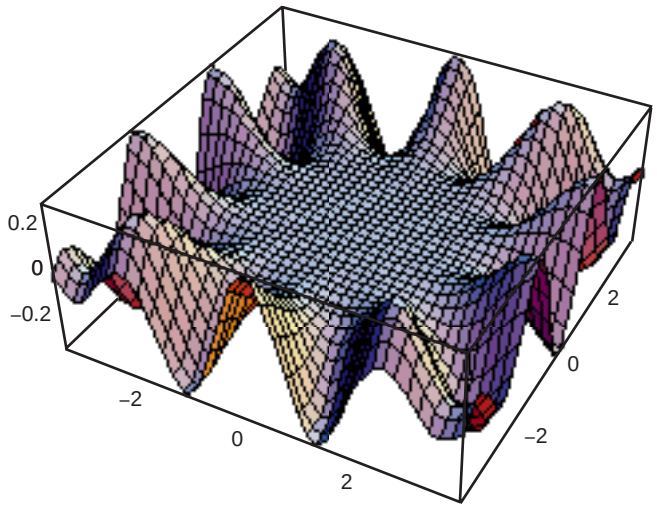

Fig. 1. Three-dimensional EM-field presentation of $TE_{5,0,\delta}$.

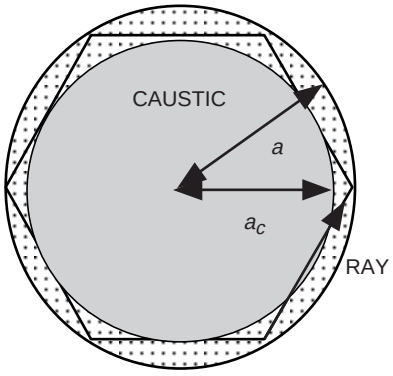

Fig. 2. Ray-tracing model of WG modes.

For the cylindrical dielectric structure, the well-known H_z field expression is given as

$$H_z = P(r)F(\phi)Z(z) = A_{mn}J_n(k_r r)e^{-in\phi}e^{-ik_z z} \tag{2}$$

where J_n is the Bessel function of order n, and k_r and k_z are the r- and z-direction propagation constant or wave number in the dielectric, respectively, and are related by $k_r^2 + k_z^2 = \varepsilon\mu\omega^2 = k^2$. The flux of energy at azimuthal direction (Poynting vector) S_Φ can be expressed from Eqs. (1) and (2) as the following:

$$S_\phi(r) = \frac{1}{2}E_r \times H_z \propto \frac{J_n^2(k_r r)}{r} \tag{3}$$

Note that Bessel function $J_n(x)$ starts to be an oscillating function when $x = n$, so that, from Eq. (2), the caustic radius can be expressed as

$$a_c = \frac{n}{k_r} \tag{4}$$

When r is larger than a_c and less than a, there is a field oscillation between a_c and a, and when r is less than a_c or larger than a, the field becomes evanescent. There are also traveling-wave-type oscillations along the circular-shaped disk in the azimuthal direction and standing-wave-type oscillations between two ends of the disk in the axial direction.

For high-order WG modes, the field oscillating area between the caustic and the boundary is too small to allow an entire mode to exist in the DR disk in the radial direction, and there is no zero point of $J_n(k_1 r)$ along the radial direction inside the resonator. In this particular case, the peak of the WG-mode energy distribution is very close to the resonator–air boundary surface. Therefore, the DR resonator becomes a quasi-surface traveling-wave resonator ($m = 0$). In comparison with other resonant modes inside of the resonator ($m \geq 1$), which confine most of the energy inside of the resonator, the modes in the surface traveling-wave resonator provide a better opportunity for coupling to transmission lines, and the performance of the Q-factor greatly depends on the smoothness of the DR disk surface. Azimuthal mode numbers n for this high-order WG-mode resonator can be estimated by

$$n = \frac{2\pi a}{\lambda_{\text{effective}}} = \frac{2\pi a \times f\sqrt{\varepsilon_r}}{c} \tag{5}$$

where c is the speed of light in the free space and f is the resonant frequency.

The calculation results obtained from Eq. (5) were compared with those of other more complicated models based on full-field analysis when the radial mode number is zero [3,4]. The comparisons are shown in Tables 1 and 2 for the cases $\varepsilon_r = 9.6$ and 36. These good-agreement results promise that simple estimating expressions, as shown in Eq. (5), could give pretty good theoretical prediction for high-order WG-mode numbers.

III. Coupling Between the Dielectric Resonator and the Transmission Medium

First of all, to determine the coupling method and direction, the cavity Q-factors of different mode types and mode-sequence numbers were calculated by finite-element tool. In the calculation, we assume a dielectric cylindrical disk ($\varepsilon_r = 30$) is sitting at the center of an aluminum cavity ($R = 2$ cm and $H = 0.84$ cm). From the results shown in Fig. 3, we find that pure modes like TE and TM generally

Table 1. Comparison of results calculated from Eq. (5) with other models, ε_r = 9.6, $2a$ = 19.00 mm.

Resonant frequency, GHz	Modes in [3] and [4]	Azimuthal mode number n calculated by Eq. (5)
28.467	$TE_{18,0,0}$	17.5492894
30.688	$TE_{19,0,0}$	18.9184879
32.886	$TE_{20,0,0}$	20.2735073
34.99	$TE_{21,0,0}$	21.5705778

Table 2. Comparison of results calculated from Eq. (5) with other models, ε_r = 36, $2a$ = 14.80 mm.

Resonant frequency, GHz	Modes in [3] and [4]	Azimuthal mode number n calculated by Eq. (5)
31.536	$TE_{29,0,0}$	29.3256867
33.287	$TE_{31,0,0}$	30.9539616
34.978	$TE_{33,0,0}$	32.5264418
36.586	$TE_{35,0,0}$	34.0217394

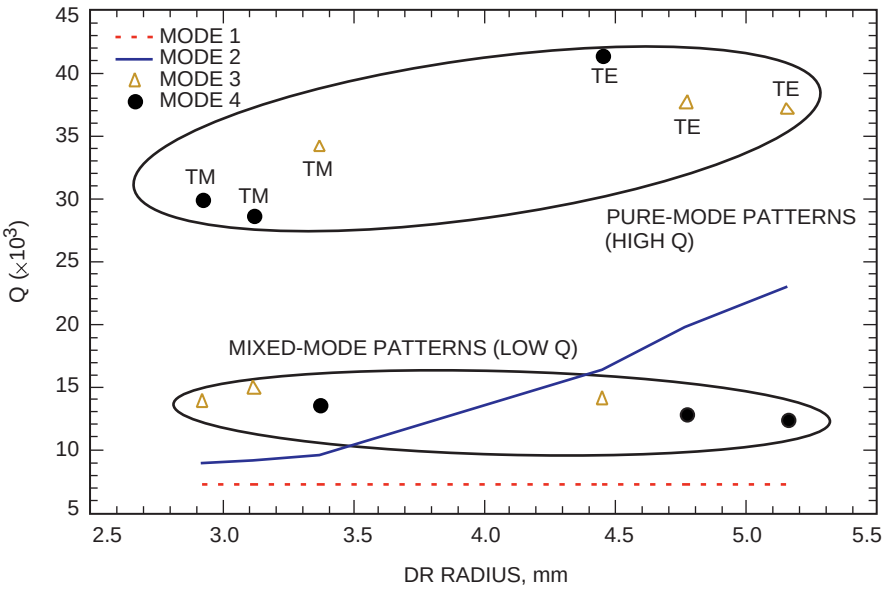

Fig. 3. A comparison of cavity Q-factors between different modes.

have higher Q as compared with other mixed modes and that TE modes have higher Q and are likely to appear among higher-order modes in a larger sized disk. Through later experimental investigation, we found that this result also applies to the case of imperfect cavity enclosure of cylindrical DRs.

Figure 4 shows the H-field and E-field of TE modes and the coupling between a cylindrical high-relative-dielectric-constant dielectric resonator and two microstrip lines mounted on a low-loss dielectric substrate. To couple TE modes in the dielectric resonator, the energy transfer occurs in the magnetic field by using magnetic dipole (tiny loop wire), TE-mode waveguide, or a microstrip line that is mounted in the same plane as the DR disk. In the case of filter design, the distance between the coupling transmission media and the DR disk always has a trade-off between insertion loss and loaded Q. Figure 5 shows the trends of insertion loss and loaded Q in a magnetic-loop-coupling 8- to 12-GHz (X-band) DR filter when the distance between the coupling loop and the DR ($\varepsilon_r = 30$) disk is variable. From this graph, we learn that weak coupling provides low insertion loss and low Q; in contrast, strong coupling provides high insertion loss and high Q. Critical coupling, which is the midway between weak and strong coupling by taking half of the input energy, is preferred in many design cases.

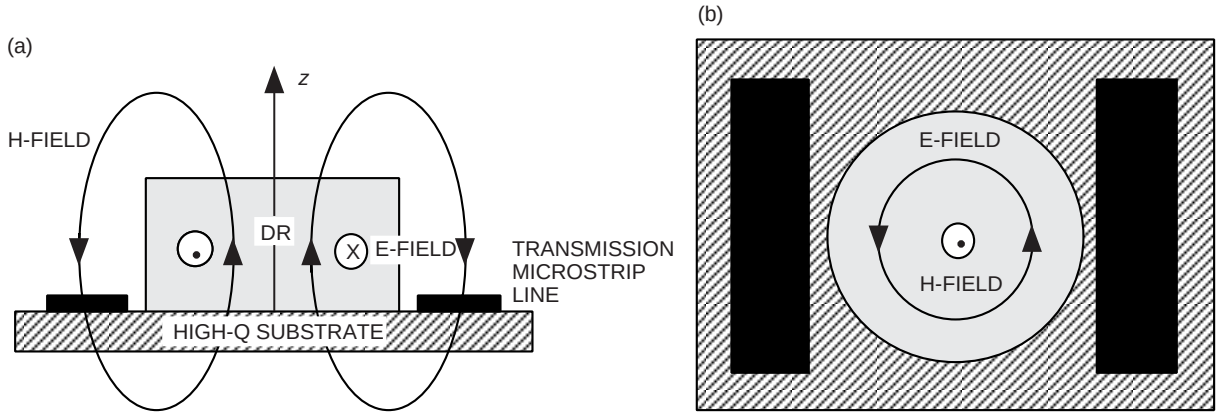

Fig. 4. The H-field and E-field of the TE modes and the coupling between the DR and the microstrip lines: (a) side view and (b) top view.

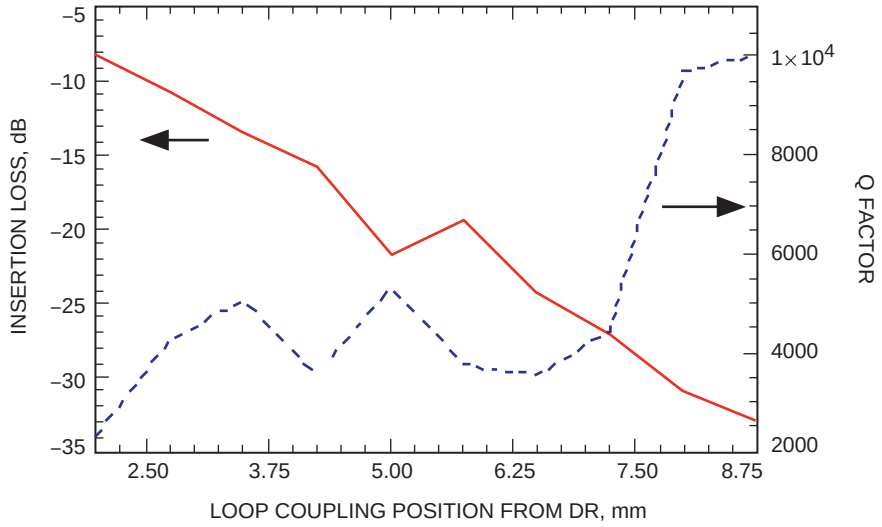

Fig. 5. Trends of insertion loss and loaded Q in an X-band filter when the distance between the DR and the loop wire is variable.

IV. Design and Performance of the X-band DR Filter

We also designed and fabricated an X-band filter by placing a 10-mm-in-diameter by 4-mm-in-height dielectric-constant ($\varepsilon_r = 30$) ceramic cylindrical disk at the center of an aluminum cavity with a size three times that of the DR disk. Using a design tool based on the finite-element method, we found that the $TE_{4,0,0}$ mode has a frequency of 10 GHz and that more than 90 percent of the energy can be confined in the disk. To realize optimum mode matching, a tiny wire loop probe was used for both mode excitation and coupling. By carefully adjusting the wire loop, critical coupling was achieved. At critical coupling, the insertion loss was minimized and the external Q of the filter was optimized. Figure 6 shows the filter structure as well as the x–z and x–y plane field distributions of the $TE_{4,0,0}$ mode in the disk and the cavity. The measured bandwidth of this filter is 2 MHz at 9.56 GHz with a 6-dB insertion loss and a Q of about 5,000 (Fig. 7). This filter allows us to use up to 6-km fiber in the OEO loop for a minimum 50-dB spurious mode suppression ratio.

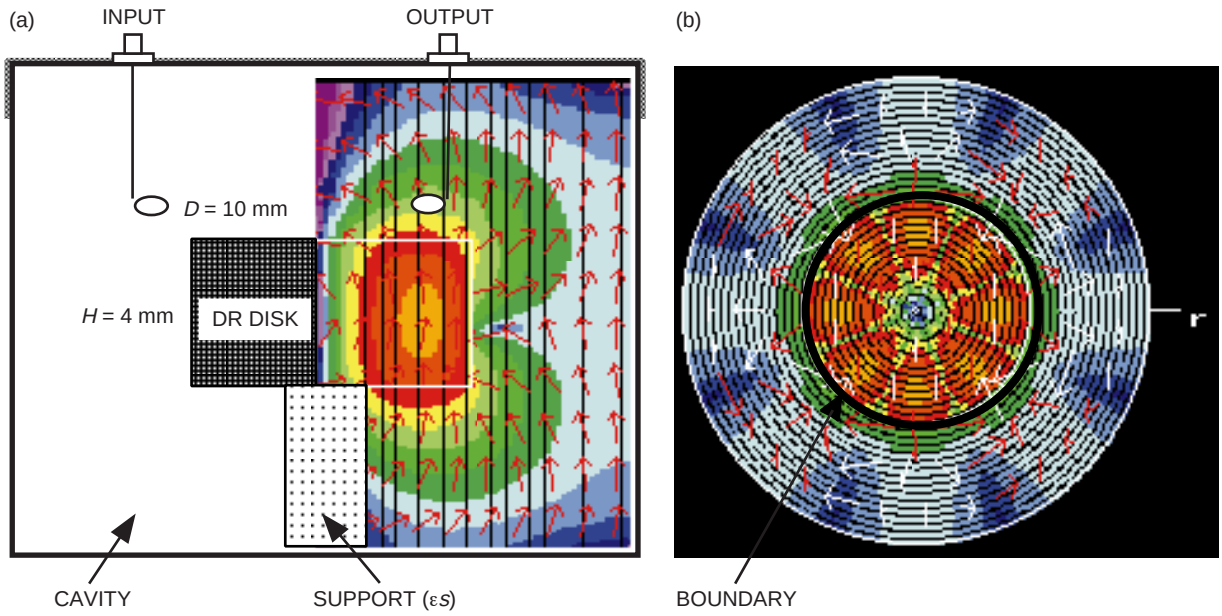

Fig. 6. The X-band DR filter: (a) the structure and the field distribution of the $TE_{4,0,0}$ operating mode in the x–z plane and (b) the field distribution of the $TE_{4,0,0}$ operating mode in the x–y plane.

V. Design and Performance of the Millimeter-Wave Band Filter

The planar structure of the proposed configuration of the millimeter-wave filter is shown in Fig. 8. The total cost of this filter is less than $20. Instead of using conventional straight-type microstrip line, we used curved strip lines for both mode excitation and coupling. The advantage of this structure is that the position of the DR disk between strip lines has high freedom. One printed circuit board could meet variable design requirements of insertion loss and loaded Q by placing different sized DRs. To reduce the reflection from the end of microstrip lines and standing waves in the transmission lines, two high-frequency 50-Ω terminations were mounted at the ends of the microstrip lines.

Rogers Duroid 5800 substrate was used in the circuit, which has a dielectric constant of $\varepsilon_s = 2.2$ and the lowest dissipation factor, $\tan\delta$ (0.0009). We chose an Ube ceramic cylindrical-type disk, which has a dielectric constant, ε_r, of 24 and a size of 6 mm (D_{outer}) × 3.71 mm (H) × 2 mm (D_{inner}), as our dielectric resonator. The Ube ceramic resonator with a center hole has a very high Q-factor (more than 17,000 at 10 GHz; an expected 5,000 at 30 GHz), a good temperature coefficient (+1 ppm/deg C), and flexibility of mounting on the substrate.

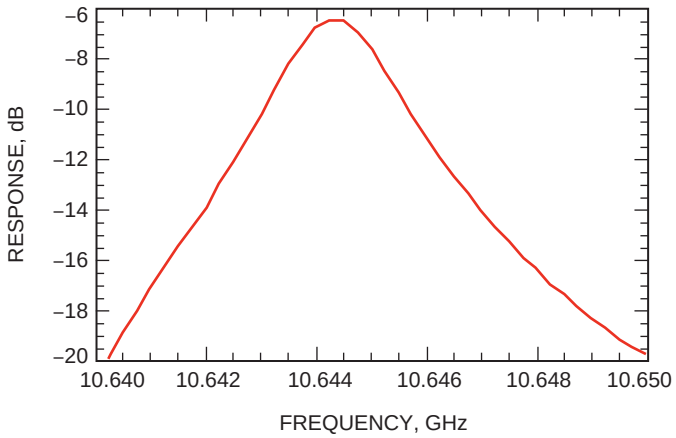

Fig. 7. The measured S_{12} of the X-band DR filter.

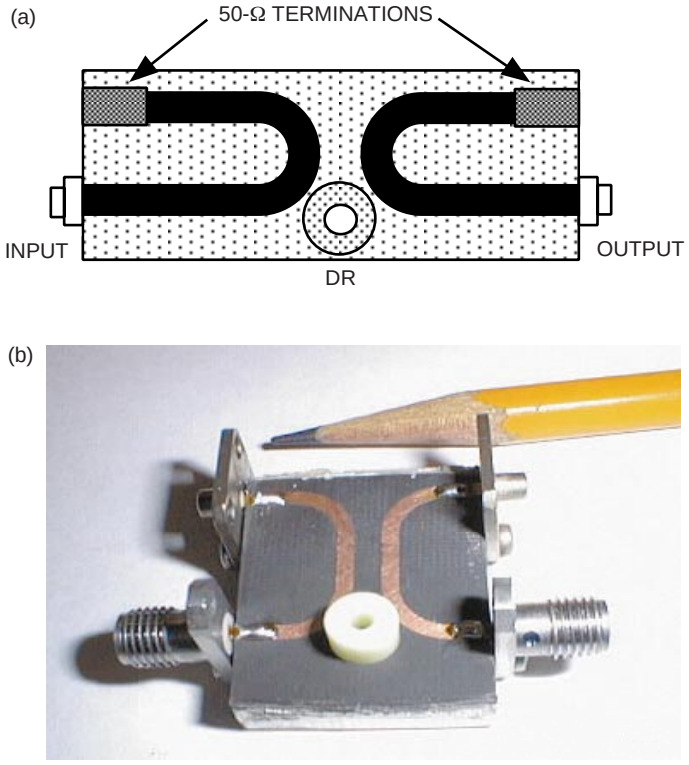

Fig. 8. Millimeter-wave filter (a) structure and (b) photograph.

The ratio of width, w, of the strip line and the thickness, h, of the substrate determine the impedance of the transmission lines. From the graph shown in Fig. 9, which was calculated from an equation in [8] for making a 50-Ω transmission line, the ratio of w/h should be 3 for this particular substrate ($\varepsilon_s = 2.2$).

Since the DR is directly mounted on the substrate and there is no additional support between the DR and the substrate for size and cost reduction, the thickness of the low-loss dielectric substrate may directly affect the performance of the loaded Q or bandwidth of the filter. By using Trans-Tech resonator-design software, CARD, the loaded Q of the filter and the coupling coefficient between the DR and the microstrip-line versus the dielectric-substrate thickness were calculated. Figure 10 shows the calculation

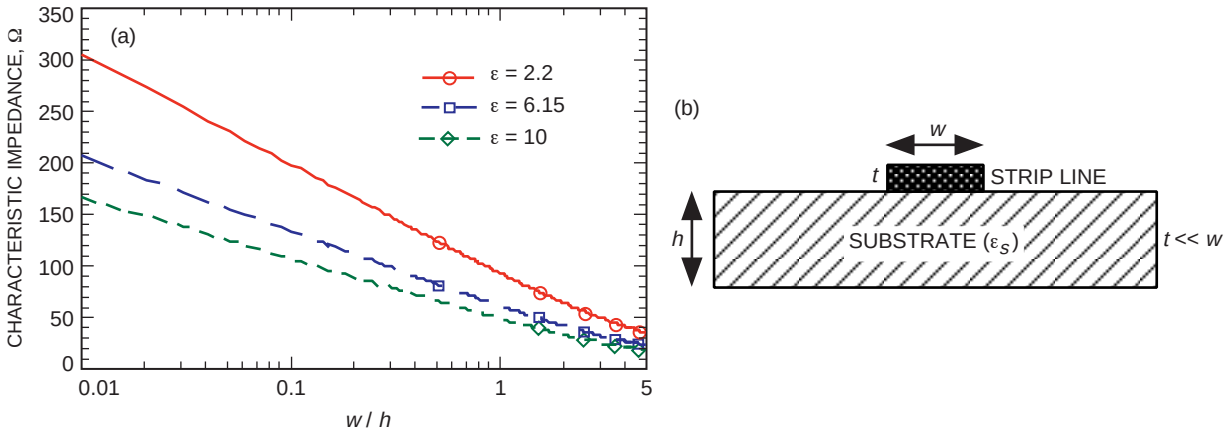

Fig. 9. The width of the 50-Ω microstrip transmission lines: (a) result of calculations and (b) structure.

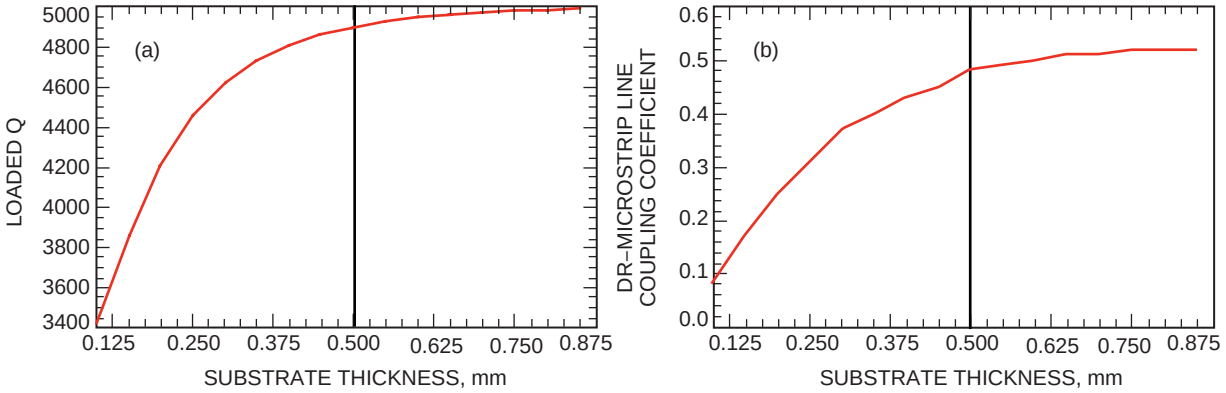

Fig. 10. Optimizing the dielectric substrate thickness: (a) the calculated loaded Q of the filter versus the dielectric substrate thickness and (b) the coupling coefficient between the DR and the microstrip line versus the dielectric substrate thickness.

results, and we found that a 0.5-mm substrate thickness is a proper choice to obtain a high loaded Q and keep a relatively high coupling coefficient level.

The comparison of modes from 15 GHz to 20 GHz between same-sized DR disks with and without center holes is shown in Fig. 11. The inner hole tends to increase the free spectrum range (FSR), reduce other low-Q modes, and shift the resonant frequencies.

The measured transmission response, S_{12}, of the filter is shown in Fig. 12. The achieved 3-dB bandwidth is 10.5 MHz (the loaded Q is about 3,000) or 0.03 percent at 31.5 GHz with a 3-dB insertion loss and more than a 25-dB band-stop attenuation.

From the evaluation of Eq. (4), the mode for the resonant frequency of 31.5 GHz should be $TE_{10,0,\delta}$, which is a high-order WG mode. The contour plot of energy density of this mode, which is calculated by Eq. (3), is shown in Fig. 13. From this figure, we can see that, although the peak of energy density still remains inside of the resonator, quite a large percentage of energy exists around the boundary outside of the resonator. This energy is relatively easier to couple by microstrip lines.

Figure 14 shows the trend of bandwidth and insertion loss when the coupling is becoming weaker. In particular applications, such as with OEO, if the insertion loss could be compensated by amplifiers, a higher Q or narrower bandwidth filter could be achievable.

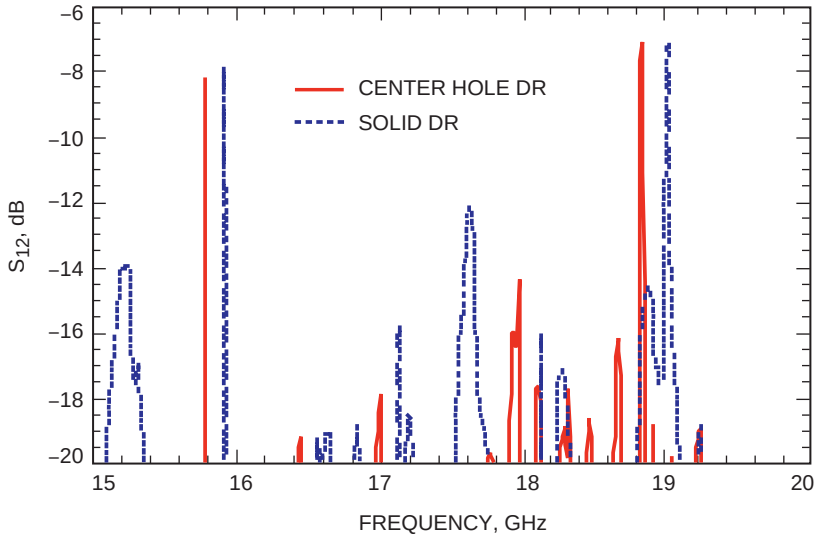

Fig. 11. Mode separations of DRs with and without a center hole.

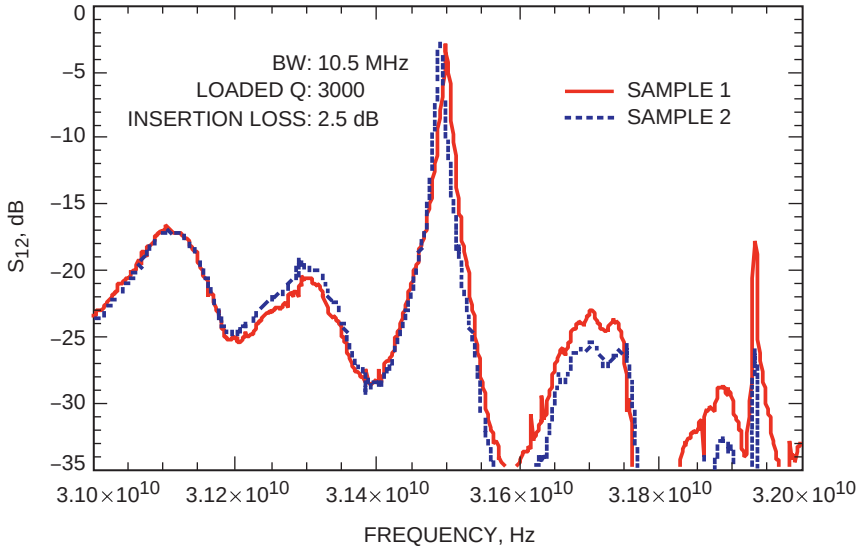

Fig. 12. Measured S_{12} of the millimeter-wave filter.

VI. Conclusion

A low-cost high-Q ultra-narrow-bandwidth millimeter-wave dielectric-resonator loaded filter utilizing whispering-gallery (WG) modes was reported on in this article. To our knowledge, this filter has the narrowest bandwidth among existing millimeter-wave filters. This filter will be used in a millimeter-wave optoelectronic oscillator for mode selection. The stop-band attenuation can be further increased by employing a number of resonators (sections) with a cascade connection.

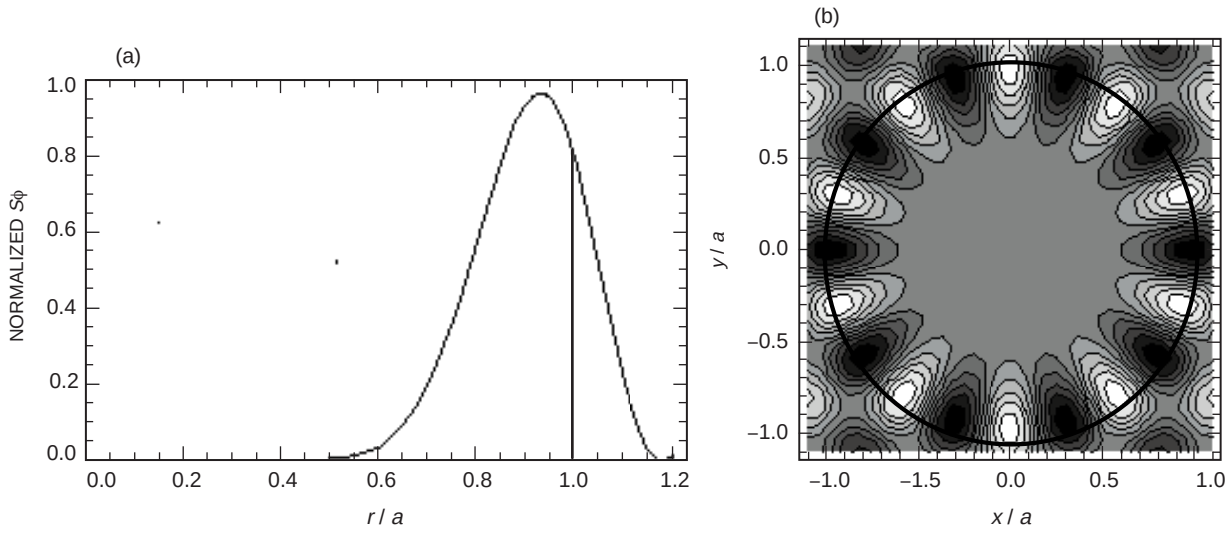

Fig. 13. The calculated energy density of the $TE_{10,0,\delta}$ operating mode for the filter: (a) normalized and (b) distribution.

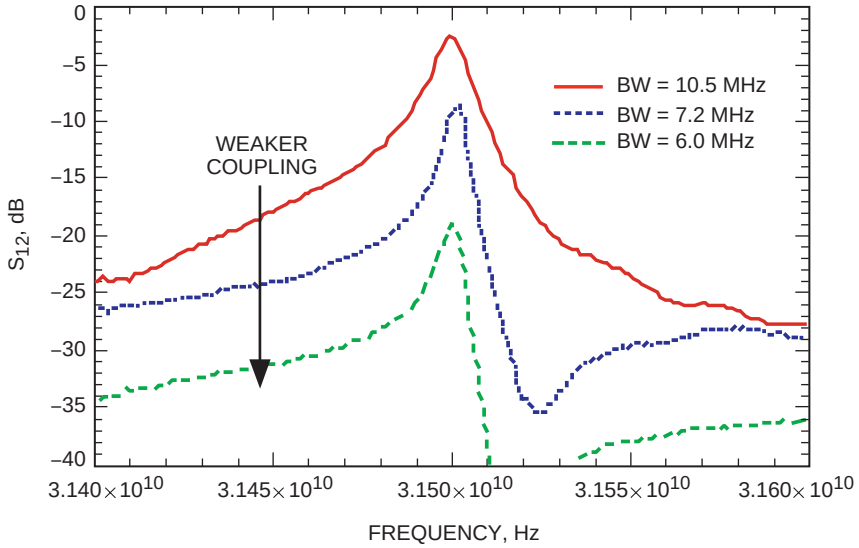

Fig. 14. The filter resonse for critical and weak coupling.

Acknowledgments

We thank R. T. Wang for his help in finite-element computation and V. S. Ilchenko and J. Dick for many helpful discussions.

References

[1] X. S. Yao and L. Maleki, "Optoelectronic Microwave Oscillator," *J. Opt. Soc. Am. B*, vol. 13, pp. 1725–1735, August 1996.

[2] S. Cohn, "Microwave Bandpass Filters Containing High-Q Dielectric Resonators," *IEEE Trans. Microwave Theory and Technology*, vol. MTT-16, pp. 218–227, April 1968.

[3] C. Vedrenne and J. Arnaud, "Whispering-Gallery Modes of Dielectric Resonators," *Proc. Inst. Elec. Eng.*, pt. H, vol. 129, pp. 183–187, August 1982.

[4] X. H. Jiao, P. Guillon, L. A. Bermudez, and P. Auxemery, "Whispering-Gallery Modes of Dielectric Structures: Applications to Millimeter-Wave Bandstop Filters," *IEEE Trans. MTT*, vol. MTT-35, no. 12, pp. 1169–1175, December 1987.

[5] D. Cros, F. Nigon, P. Besnier, M. Aubourg, and P. Guillon, "Whispering Gallery Dielectric Resonator Filters," *IEEE MTT-S International Microwave Symposium*, vol. 2, pp. 603–606, 1996.

[6] D. Kajfez and P. Guillon, eds., *Dielectric Resonators*, Artech House: Dedham, Massachusetts, 1986.

[7] T. Hiratsuka, T. Sonoda, K. Sakamoto, and Y. Ishikawa, "K-Band Planar Type Dielectric Resonator Filter With High-ε Ceramic Substrates," *1998 IEEE MTT-S International Microwave Symposium Digest*, vol. 3, pp. 1311–1314, June 1998.

[8] I. J. Bahl and P. Bhartia, *Microwave Solid State Circuit Design*, New York: Wiley, 1988.